Determination of aperture structure and fluid flow in a rock fracture by a high-resolution numerical modeling on the basis of a flow-through experiment under confining pressure

著者	Watanabe Noriaki, Hirano Nobuo, Tsuchiya Noriyoshi
journal or publication title	Water Resources Research
volume	44
number	6
page range	W06412
year	2008
URL	http://hdl.handle.net/10097/53090

doi: 10.1029/2006WR005411

Determination of aperture structure and fluid flow in a rock fracture by high-resolution numerical modeling on the basis of a flow-through experiment under confining pressure

Noriaki Watanabe,[1] Nobuo Hirano,[1] and Noriyoshi Tsuchiya[1]

Received 7 August 2006; revised 24 January 2008; accepted 25 February 2008; published 17 June 2008.

[1] A numerical model incorporating experimentally determined fracture surface geometries and fracture permeability is proposed for characterizing aperture structures and fluid flow through rock fractures under confining pressures. The model was applied to artificially created granite tensile fractures with varying shear displacements (0–10 mm) and confining pressures (10–100 MPa). The findings of the study were consistent with those obtained previously, which characterized experimentally determined contact areas and changes in shear stress during the shear process. While the confining pressures considered herein are higher than those of previous studies, experimentally obtained fracture permeability is important for understanding subsurface flow, specifically the fluid flow characteristics in aperture structures under different confining pressures. Development of preferential flow paths is observed in all aperture structures, suggesting that the concept of channeling flow is applicable even under high confining pressures, as well as the existence of 3-D preferential flow paths within the subsurface fracture network.

Citation: Watanabe, N., N. Hirano, and N. Tsuchiya (2008), Determination of aperture structure and fluid flow in a rock fracture by high-resolution numerical modeling on the basis of a flow-through experiment under confining pressure, *Water Resour. Res.*, *44*, W06412, doi:10.1029/2006WR005411.

1. Introduction

[2] In the Earth's crust, rock fractures are thought to play an important role in both fluid flow and material/heat transport within these fluids. Consequently, fracture permeability is expected to be greater than matrix permeability in fractured rock. In fact, the results of flow-through experiments in various types of granite fractures indicated that fracture permeability was usually considerably greater than matrix permeability, even under the relatively high confining pressures (normal stresses) of 10–100 MPa, and correspondingly, at relatively great depths of 400–4000 m [*Watanabe et al.*, 2006b, 2006c]. The experimental observations suggest that interactions among flow and transport phenomena between shallow- and deep-seated fracture networks are therefore likely within the Earth's crust, unless the networks are completely isolated from each other. Understanding of fluid flow through rock fractures under a wide range of confining pressures, exceeding the range of previous practical interest for water resources issues, has become a fundamental issue of considerable importance, not only for engineering activities targeting depths of several-thousand meters (e.g., developments of oil/gas fractured reservoirs), but also for relatively shallow activities targeting several hundreds of meters (e.g., geological disposal of high-level radioactive waste). For instance, the Japanese Atomic Energy Agency (JAEA) has constructed an underground laboratory (tunnels) in the Mizunami granite body in Gifu, Japan, for regional groundwater flow survey at depths exceeding 1000 m (at confining pressures of more than 25 MPa) in order to examine geological disposal of high-level radioactive wastes. Lab-scale studies of fluid flow in rock fractures for a wide range of confining pressures are needed to interpret field observations and to develop a realistic model of a 3-D subsurface flow system.

[3] Rock fractures are characterized as having a heterogeneous aperture structure and are characterized as having a three-dimensional distribution of local apertures formed by rough surfaces that, depending on the confining pressure, are in partial contact with each other with, presumably, preferential flow paths (i.e., the occurrence of channeling flow) in the aperture structure [*Brown*, 1987; *Tsang and Tsang*, 1989; *Durham*, 1997; *Brown et al.*, 1998; *Bruderer-Weng et al.*, 2004]. In general, fracture permeability not only changes with confining pressure, but also with shear displacement [*Raven and Gale*, 1985; *Esaki et al.*, 1999; *Chen et al.*, 2000; *Gutierrez et al.*, 2000; *Plouraboué et al.*, 2000; *Olsson and Barton*, 2001]. The changes indicate that the aperture structures of rock fractures and the resulting fluid flow are affected by both confining pressure and shear displacement. It is therefore important to investigate the heterogeneous nature of the aperture structures of rock fractures and the resulting fluid flow in these fractures as a function of geological conditions such as shear displacement and confining pressure. In previous studies, fluid flows through numerically generated aperture structures have been studied extensively, and channeling flows have been observed [*Unger and Mase*, 1993; *Pyrak-Nolte and*

[1] Graduate School of Environmental Studies, Tohoku University, Aoba-ku, Sendai, Miyagi, Japan.

0043-1397/08/2006WR005411

Morris, 2000; *Lespinasse and Sausse*, 2000; *Sausse*, 2002; *Koyama et al.*, 2006; *Matsuki et al.*, 2006]. However, the relationships between numerical observations and geological conditions, particularly with respect to confining pressures, have not been accurately clarified due to difficulties associated with demonstrating model robustness through experimental observations under equivalent conditions. This failure to incorporate experimental observations into numerical techniques means that numerical observations, such as observations of channeling flow, can only rarely be applied to rock fractures under actual geological conditions. Since the possible aperture structure (possible the magnitude of local apertures and the number of contact points, etc.) for a rock fracture depends on both shear displacement and confining pressure and is reflected by fracture permeability, the fluid flow under specific conditions in the aperture structure can be determined bases on fracture permeability measurements under varying conditions, or by experimental methods that do not employ numerical techniques.

[4] Casting techniques, for example, have been used to characterize the aperture structures of rock fractures using casting agents (e.g., Wood's metal) [*Hakami and Larsson*, 1996; *Kostakis et al.*, 2003; *Konzuk and Kueper*, 2004; *Yasuhara et al.*, 2006]. Since it is not necessary to separate the two fracture surfaces, these techniques can be used to produce undisturbed aperture structures. In addition, the casting technique can achieve precise determination of aperture structures by being combined with the X-ray computed tomography (CT) technique [*Montemagno and Pyrak-Nolte*, 1999]. However, casting techniques are not suitable for the investigation of aperture structures under varying conditions since they are destructive and contaminative. On the other hand, recent X-ray CT techniques with no casting agent can be used to determine aperture structures without the aforementioned problems [*Bertels et al.*, 2001; *Polak et al.*, 2004]. However, performing this technique is difficult due to the high costs involved and the potential technical difficulties associated with applying the technique to rock fractures under relatively high confining pressures (e.g., more than 10 MPa). Although other experimental methods have been proposed, no practical method exists for determining the aperture structures, and consequently the fluid flow, in a rock fracture under varying conditions including high confining pressures.

[5] The objectives of the present study are to propose a practical numerical technique for incorporating the results of flow-through experiments in the determination of aperture structures and the resulting fluid flow in rock fractures under a wide range of confining pressures. In addition, the results provide fundamental insights into the heterogeneous nature of aperture and flow structures in rock fractures with various shear displacements (0–10 mm) under various confining pressures exceeding those of previous practical interest for water recourses issues (10–100 MPa). First, the previously performed flow-through experiments for artificially created granite tensile fractures are described [*Watanabe et al.*, 2006b]. Second, a numerical model is proposed based on a flow-through experiment, and this model is applied to the generated fractures.

2. Flow-Through Experiment

[6] Cylindrical samples (100 mm in diameter and 150 mm in length) of Inada mediu ed Granite (Ibaraki, Japan) containing single tensile fractures (100 mm × 150 mm) were used together with measurements of fracture surface geometries for the flow-through experiments to measure fracture permeability under various confining pressures. A 200 mm cubic granite block was fractured using a wedge to create a tensile fracture, which was then given a prescribed shear displacement. The block, which was fixed with concrete, was cored and cut to the prescribed dimensions. To investigate the effects of shear displacement on the aperture structures of a rock fracture and the resulting fluid flow, samples were prepared that contained either single tensile fractures with shear displacements of 1, 3, 5, and 10 mm (samples NC05, NC07, NC06, and NC09) or no shear displacement (0 mm; samples NC01, NC02, and NC03).

[7] Before conducting flow-through experiments, measurements of fracture surface geometries were performed for each fracture using laser-scanning equipment (positioning accuracy: ±20 μm, asperity height resolution: 10 μm). Each fracture was separated into two surfaces, and fracture surface geometries were measured for each surface using a 250-μm square grid system (400 × 600 data points). Fractal analysis of the obtained data was then performed to assess the fractal nature of the samples [*Brown*, 1987; *Tsuchiya and Nakatsuka*, 1995, 1996; *Power and Durham*, 1997]. The results of fractal analysis revealed fractal dimensions of 1.40–1.59 for the profiles of the fracture surfaces. The results suggested that the fractures tested in the present study were an acceptable substitute for natural rock fractures.

[8] Flow-through experiments were performed under confining pressures of 10–100 MPa using a Rubber-Confining Pressure Vessel (R-CPV) experimental system developed by *Hirano et al.* [2005] (Figure 1). The R-CPV with the sample was placed in a pressing machine (maximum load: 25,000 kg). By controlling the load of the pressing machine, a prescribed confining pressure could be applied to the fracture of the sample. Distilled water (room temperature) was pumped into the R-CPV, and the differential pressure between the inlet and outlet sides of the fracture was measured using a differential pressure gauge. In addition, the flow rate was measured using an electronic balance. Since the relationships between the flow rate and the differential pressure were linear in the experiments, the hydraulic aperture, and consequently, the fracture permeability, could also be calculated for individual fractures at specific confining pressures on the basis of the cubic law assumption [*Brown*, 1987; *Chen et al.*, 2000; *Matsuki et al.*, 2006].

[9] The fracture permeability in the direction perpendicular to shear displacement under confining pressures of 10–100 MPa is shown for different shear displacements (Figure 2). The fracture permeability for a shear displacement of 0 mm was the lowest among the obtained shear displacements (Figure 2a). While the fracture permeability differed slightly among the three samples, significant decreases were only observed when the confining pressure was increased under relatively low pressure (approximately 10–50 MPa) and remained considerably higher than the matrix permeability of 10^{-19}–10^{-18} m^2, even at a confining pressure of 100 MPa [*Takahashi et al.*, 1990]. Conversely, for shear displacements greater than 1 mm, the fracture

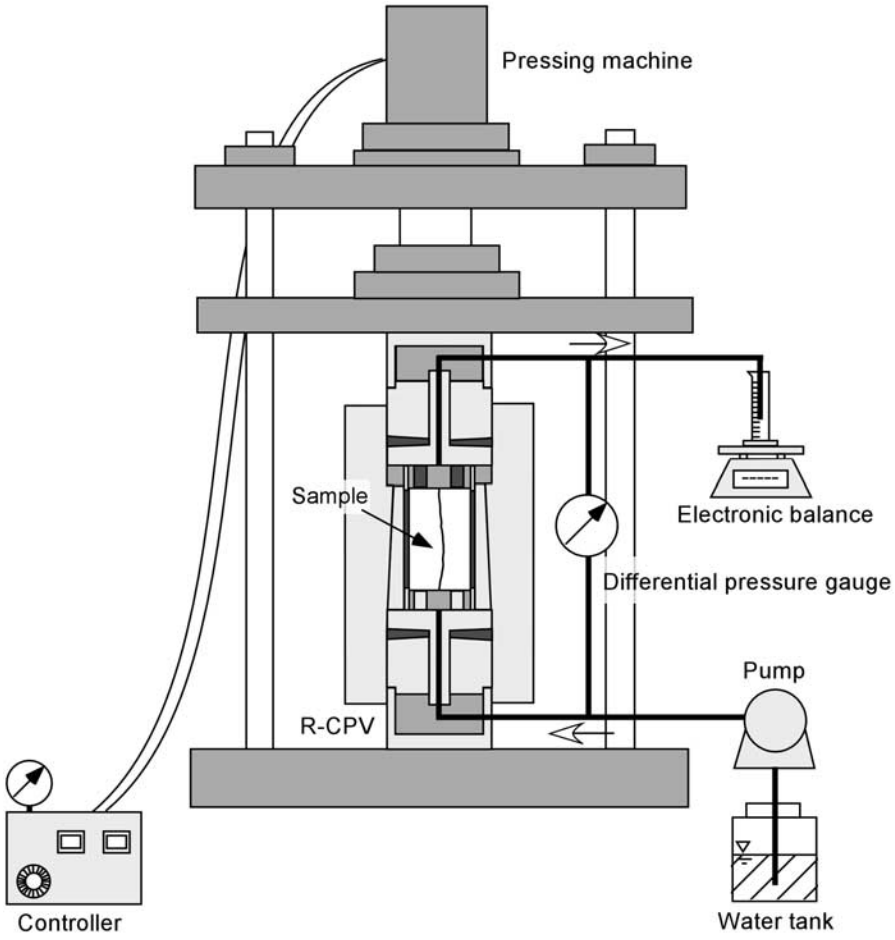

Figure 1. Flow-through experiment system with the Rubber-Confining Pressure Vessel (R-CPV) developed by *Hirano et al.* [2005].

permeability was several orders of magnitude greater than that observed for a shear displacement of 0 mm, increasing with an increase in shear displacement (Figure 2b). While the fracture permeability for a shear displacement of 1 mm decreased with an increase in confining pressure, the fracture permeability for shear displacements exceeding 3 mm only decreased under relatively low pressures (approximately 10–30 MPa).

3. Numerical Modeling on the Basis of a Flow-Through Experiment

3.1. Outline

[10] In the present study, a numerical model incorporating experimentally measured fracture surface geometries and fracture permeability was proposed for determining aperture structure and resulting fluid flow for rock fractures under prescribed confining pressures. The model of the aperture structure was constructed using digital data of fracture surface geometries with shear displacement. The local cubic law (LCL)-based flow-through simulation was performed using the model under the same boundary conditions as those observed in a flow-through experiment. On the basis of the flow-through simulation, the permeability of the model was evaluated using the same equations as those employed for the flow-through experiment, and the obtained permeability was compared with the experimentally obtained fracture permeability. By comparing the numerically and experimentally derived permeabilities using a modification of the model simulating the normal displacement of a rock fracture, the aperture structures and the resulting fluid flow were determined for prescribed confining pressures.

[11] The accuracy of the results obtained using the proposed technique depends on the methods used to measure the fracture surface geometries used for constructing the aperture structure and flow-though simulation. The method selected for the measurement of fracture surface geometries was capable of producing a disturbed aperture structure, because two fracture surface geometries were measured separately. Even without shear displacement, the permeability of the fractures was considerably higher than that of the rock matrix under high confining pressures, indicating the existence of a disturbance. The disturbance could have been due to the removal of small rock particles generated during fracture. However, given the objectives of the present study, no other method could be applied. Therefore careful execution of this method is necessary in order to prevent the development of a significantly disturbed aperture structure. In addition, the methods employed to model the aperture structure and simulate flow-through in the present study were also selected based

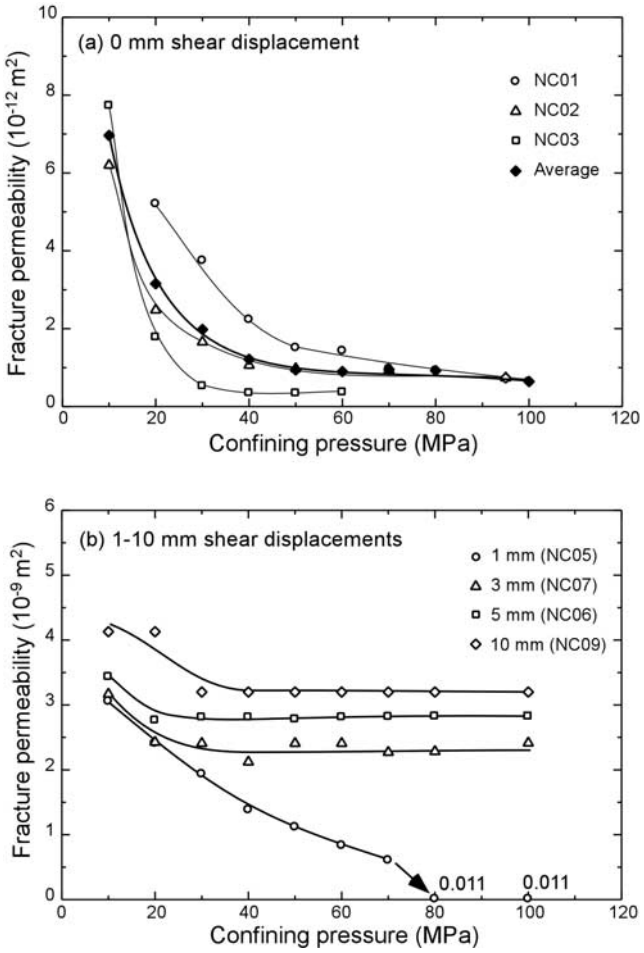

Figure 2. Experimentally obtained fracture permeability under 10–100 MPa confining pressures for artificially created granite tensile fractures (a) without shear displacement and (b) with shear displacements of 1, 3, 5, and 10 mm.

on their practicability, and these methods are described below in detail.

3.2. Construction of the Aperture Structure Model

[12] The aperture structure was modeled by representing the 2-D distribution of local apertures using a 250 μm square grid system, with local apertures represented by vertical separations between mean planes of opposite fracture surfaces. While several different representations of point-by-point local apertures exist (the normal-to-local-centerline aperture [*Ge*, 1997] and the ball aperture [*Mourzenko et al.*, 1995]), no significant differences in local apertures were observed in the relatively fine grid system of the present study. On the other hand, it has been suggested that the local apertures for the LCL-based flow-through simulation should be represented by the average separations of opposite fracture surfaces over a certain distance normal to the mean trend of the surfaces [*Oron and Berkowitz*, 1998]. However, the representation of local apertures could result in a reduction in the heterogeneity of the aperture structure.

[13] In the determination of aperture structures and resulting fluid flow for a rock fracture under prescribed confining pressures, a model with at least a single contact point with the fracture surfaces was ly constructed. The model was then modified to simulate the normal displacement (close together) of a rock fracture to match the permeability of a model with experimentally determined fracture permeability. In the modification, all local apertures were uniformly reduced. Although the deformation of actual fracture surfaces depends entirely on stress conditions, the effect of deformation was neglected, except when the asperities of the fracture surfaces came into contact, because the deformation was expected to occur predominantly at these points. In addition, by vanishing overlapped asperities, the model simulated both elastic and permanent deformations of the contacting asperities and precluded the formation of local apertures [*Brown*, 1987; *Power and Durham*, 1997; *van Genabeek and Rothman*, 1999; *Matsuki et al.*, 2006; *Watanabe et al.*, 2005, 2006a].

3.3. Flow-Through Simulation

[14] Since solving the Navier-Stokes equation that governs the 3-D flow of an incompressible and viscous fluid (water) through an aperture structure of a rock fracture is beyond the capacity of most computers, flow was approximated using a 2-D (x-y) field and by incorporating mean flow velocities across the local apertures and ignoring the tortuosity of flow across the local apertures:

$$\frac{\partial(eu)}{\partial x} + \frac{\partial(ev)}{\partial y} = 0, \tag{1}$$

where e is a local aperture, and u and v are the mean velocities in the x- and y-directions, respectively. In addition, the flow at a local point was approximated by flow through parallel plates with an aperture of e:

$$u = -\frac{e^2}{12\mu}\frac{\partial P}{\partial x}, \tag{2}$$

$$v = -\frac{e^2}{12\mu}\frac{\partial P}{\partial y}, \tag{3}$$

where μ and P are the viscosity and the pressure of the fluid, respectively. By substituting equations (2) and (3) into equation (1), the following equation (usually called the Reynolds equation) is obtained for laminar flow [*Brown*, 1987; *Mourzenko et al.*, 1995; *Yeo et al.*, 1998; *Ge*, 1997; *Oron and Berkowitz*, 1998; *Lespinasse and Sausse*, 2000; *Pyrak-Nolte and Morris*, 2000; *Sausse*, 2002; *Brush and Thomson*, 2003; *Konzuk and Kueper*, 2004; *Watanabe et al.*, 2005, 2006a]:

$$\frac{\partial}{\partial x}\left(\frac{e^3}{12\mu}\frac{\partial P}{\partial x}\right) + \frac{\partial}{\partial y}\left(\frac{e^3}{12\mu}\frac{\partial P}{\partial y}\right) = 0. \tag{4}$$

[15] Since μ is assumed to be constant, this parameter can be removed from equation (4). By solving equation (4) under given boundary conditions using the finite difference method, the 2-D velocity field could be determined by substituting the solution for pressure into the finite difference expressions of equations (2) and (3). In addition, a 2-D volumetric flow field could be determined using these velocities and local apertures. Although it has been reported that, when compared with the Navier-Stokes equation (or even with the Stokes equation), equation (4) may produce different velocities [*Mourzenko et al.*, 1995; *Ge*, 1997; *Oron*

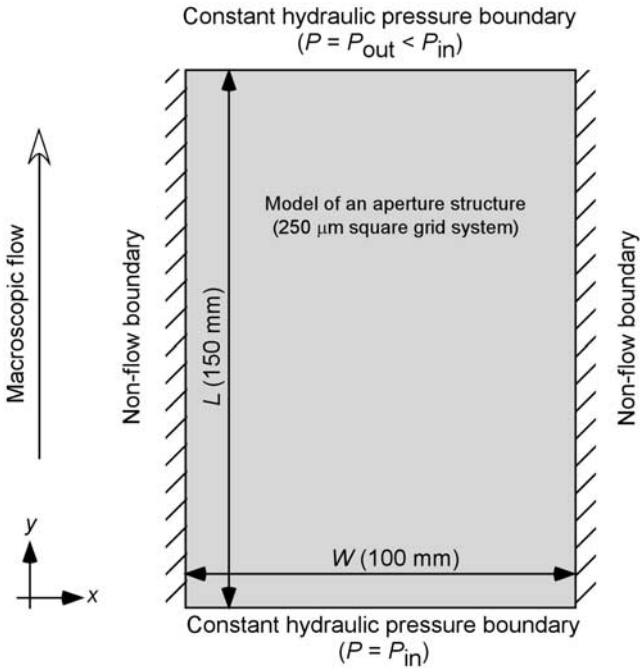

Figure 3. The boundary conditions in a flow-through simulation for a model of an aperture structure of a rock fracture.

and Berkowitz, 1998; *Brush and Thomson*, 2003; *Konzuk and Kueper*, 2004], equation (4) was used in the present study because of its practicability.

[16] Linear equations derived from a finite difference form of equation (4) were solved using a simulator, the D/SC [*Tezuka and Watanabe*, 2000], by substituting zero local apertures at contacting asperities with significantly small nonzero local apertures. This was done because pressures at the zero local apertures cannot be defined and because zero permeability might be invalid, even for the contacting asperities, due to the local apertures that were average values based on grid size. Although there was not sufficient evidence to determine valid local apertures at the contacting asperities, the permeability at these points should be less than the experimentally determined minimum fracture permeability. In the present study, the zero local apertures at the contacting asperities were substituted with 1 μm local apertures (8.3×10^{-14} m^2 local permeability), because fracture permeabilities greater than 3.4×10^{-13} m^2 were observed in the flow-through experiments. Boundary conditions were applied such that macroscopic water flow occurred in one direction (Figure 3). The boundary conditions were the same as those observed in the flow-through experiments, with constant hydraulic pressures applied to boundaries that were perpendicular to the direction of macroscopic flow. The condition of nonflow was assigned to boundaries parallel to the direction of macroscopic flow.

[17] Once the velocity field is determined, the volumetric flow rate Q can also be obtained using the following equation for determining the macroscopic flow direction:

$$Q = \int_0^W evdx, \tag{5}$$

where W is the length of the boundary perpendicular to the macroscopic flow. The hydraulic aperture (e_h) was calculated using the following equation [*Brown*, 1987; *Chen et al.*, 2000; *Matsuki et al.*, 2006]:

$$e_h = \left(\frac{12\mu Q}{W(\Delta P/L)}\right)^{1/3}, \tag{6}$$

where L is the length of the boundary parallel to the macroscopic flow and $\Delta P/L$ is the macroscopic pressure gradient. In addition, permeability (k) was calculated using the following equation:

$$k = \frac{e_h^2}{12}. \tag{7}$$

4. Results

[18] The proposed technique was applied to artificially created granite tensile fractures (100 mm $\times$ 150 mm) with shear displacements of 0, 1, 3, 5, and 10 mm under confining pressures of 10–100 MPa. For each shear displacement, aperture structures and the resulting water flow were determined for confining pressures of 10, 60, and 100 MPa using the values for fracture permeability that were determined for the fractures in the flow-through experiments (Figure 2), and from the fracture surface geometries (250 μm square grid system) that were measured for the fractures before the experiments.

[19] For a shear displacement of 0 mm, the average fracture permeability for the three fractures (samples NC01, NC02, and NC03) and the fracture surface geometries of the fracture of sample NC01 were used. For shear displacements of 1, 5, and 10 mm, the fracture permeability and fracture surface geometries of the fractures with different shear displacements (samples NC05, NC06, and NC09, respectively) were used. Finally, for a shear displacement of 3 mm, the fracture permeability of the fracture with the shear displacement (sample NC07) was used. However, due to the lack of fracture data for sample NC07, fracture surface geometries were prepared numerically by applying a shear displacement of 3 mm to the fracture surface geometries of the fracture without shear displacement (sample NC02).

[20] Images of determined aperture structures, histograms, and semivariograms (in the directions parallel and perpendicular to shear displacement) of local apertures are shown in Figures 4, 5, and 6, respectively. In addition, the statistics of the aperture structures are presented in Table 1 together with the selected fracture permeabilities and the corresponding hydraulic apertures. The images shown in the figures are only those for shear displacements of 0, 1, and 5 mm, as the images for shear displacements of 3 and 10 mm were visually similar to that obtained for 5 mm. Similarly, only samples subjected to a confining pressure 10 MPa are shown, as changes in aperture structure with increasing confining pressure simply resulted in a uniform decrease of all local apertures. Since the histograms, except for minimum (1 μm) local apertures, were highly skewed and had long tails, the lognormal distribution, rather than the Gaussian distribution, was better suited for describing the

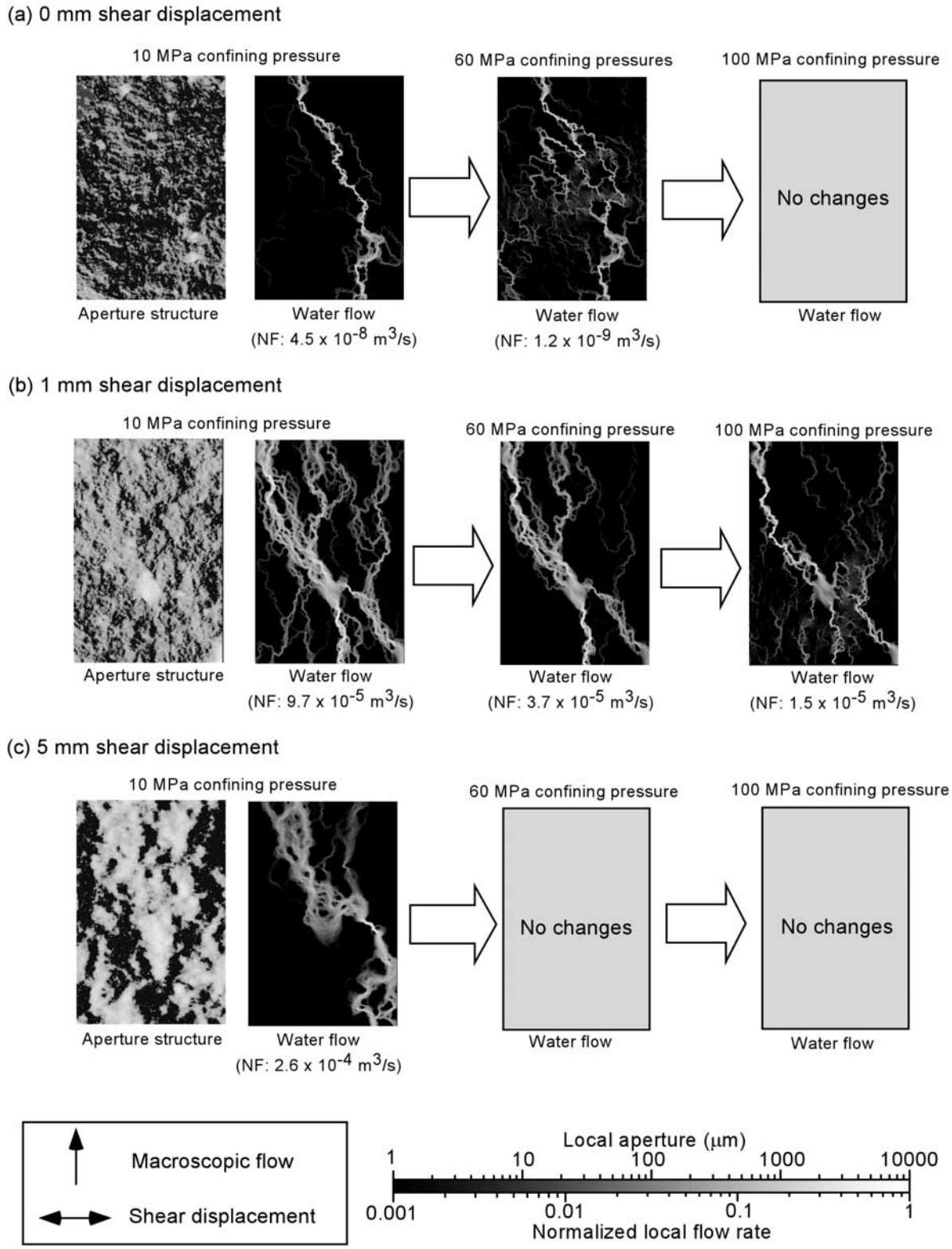

Figure 4. Numerically determined aperture structures at 10 MPa confining pressure for artificially created granite tensile fractures (a) without shear displacement, (b) with a shear displacement of 1 mm, and (c) with a shear displacement of 5 mm, together with water flow in aperture structures at confining pressures of 10, 60, and 100 MPa for the fractures. NF (normalization factor) shown below each water flow map is the maximum flow rate when a hydraulic pressure difference is 1 MPa.

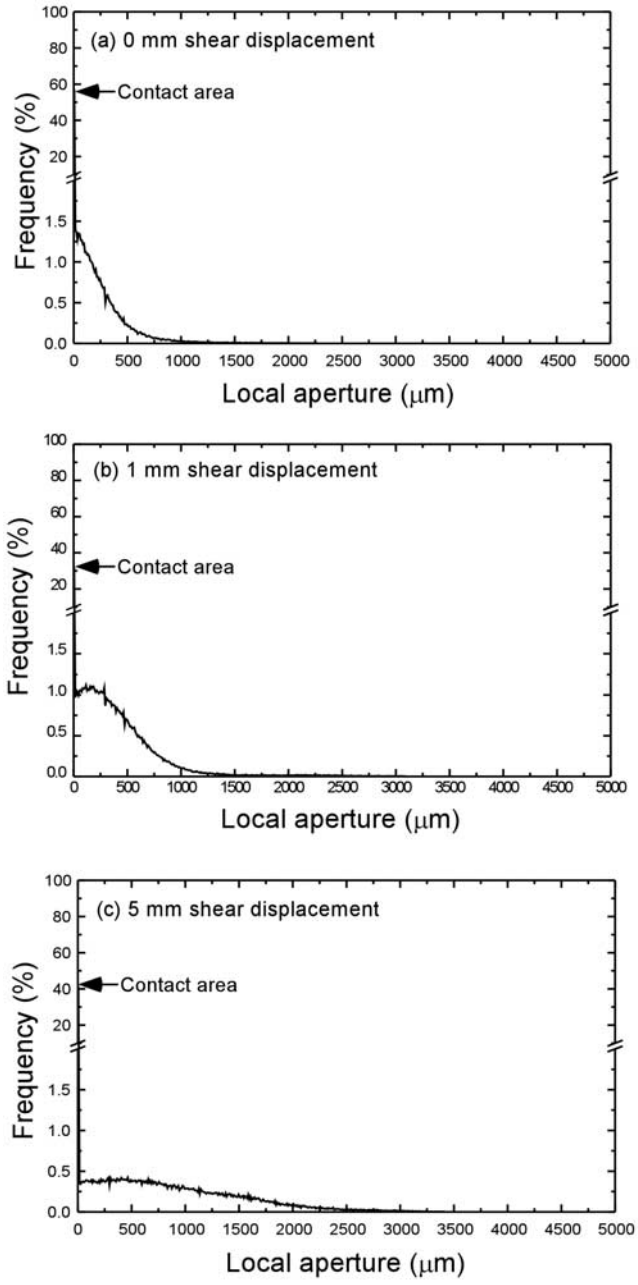

Figure 5. Histograms of local apertures for numerically determined aperture structures at a confining pressure of 10 MPa for artificially created granite tensile fractures (a) without shear displacement, (b) with a shear displacement of 1 mm, and (c) with a shear displacement of 5 mm.

distributions of local apertures. Therefore the distributions of local apertures are characterized by geometric mean apertures and geometric standard deviations calculated without the minimum local apertures, together with contact areas calculated as percentages of the minimum local apertures. The spatial correlation lengths in the directions parallel and perpendicular to the shear displacements were determined by fitting the semivariograms to the exponential model.

[21] Regarding the aperture structures for a confining pressure of 10 MPa, the histograms became wider and mean apertures became monotonically greater with increased shear displacement. Conversely, nonmonotonic changes were observed for the contact areas and spatial correlation lengths. The contact areas decreased significantly only between shear displacements of 0 and 1 mm (Figure 7). The spatial correlation lengths parallel to shear displacement increased significantly between shear displacements of 0 and 1 mm and between shear displacements of 5 and 10 mm, while those that were perpendicular to shear displacement only increased significantly between shear

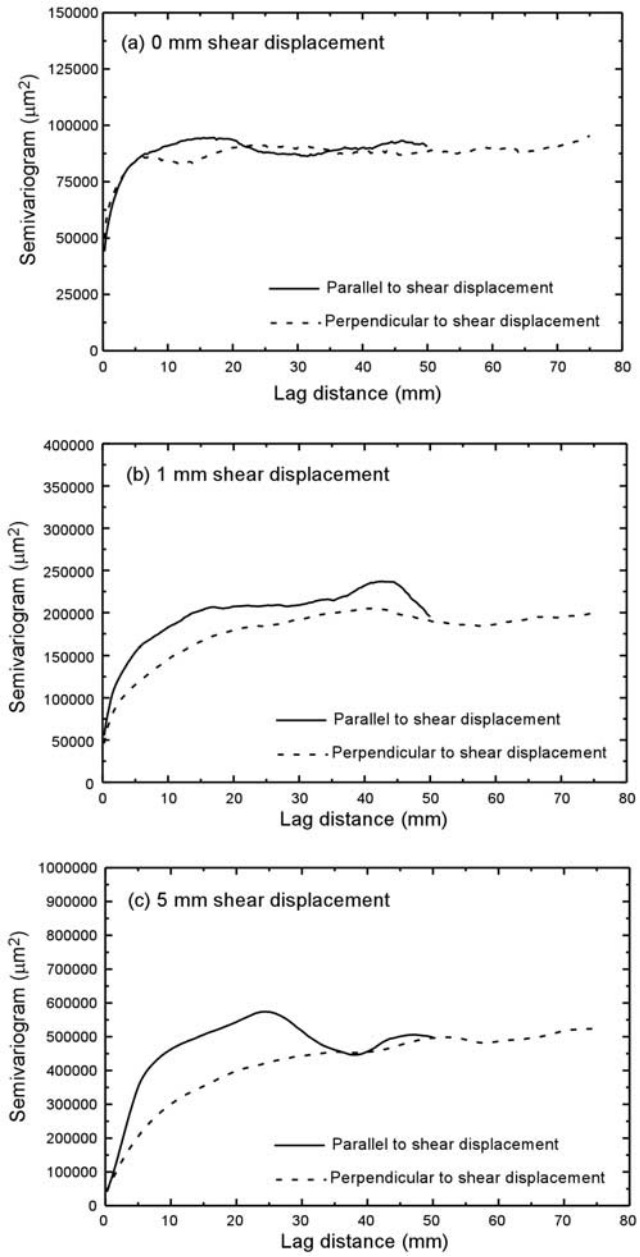

Figure 6. The semivariograms in the directions parallel and perpendicular to the shear displacement of local apertures for numerically determined aperture structures at a confining pressure of 10 MPa for artificially created granite tensile fractures (a) without shear displacement, (b) with a shear displacement of 1 mm, and (c) with a shear displacement of 5 mm.

Table 1. Experimentally Obtained Fracture Permeability, Hydraulic Apertures, and Statistics of Numerically Determined Aperture Structures at 10, 60, and 100 MPa for Artificially Created Granite Tensile Fractures Without Shear Displacement and With Shear Displacements of 1, 3, 5, and 10 mm[a]

Shear Displacement, mm	Confining Pressure, MPa	Fracture Permeability, m^2	Hydraulic Aperture, μm	Mean Aperture, μm	Standard Deviation (−)	Contact Area, %	Spatial Correlation Length, mm	
							Parallel	Perpendicular
0	10	6.9×10^{-12}	9.1	70.9	2.9	56	3	2
	60	8.0×10^{-13}	3.1	65.3	2.9	62	3	2
	100	6.5×10^{-13}	2.8	64.5	2.9	63	3	2
1	10	3.1×10^{-9}	192	196	2.3	31	12	18
	60	8.3×10^{-10}	100	171	2.3	42	12	18
	100	1.1×10^{-11}	11	75.2	3.0	66	13	18
3	10	3.1×10^{-9}	194	229	2.4	35	13	28
	60	2.4×10^{-9}	170	219	2.4	37	13	28
	100	2.4×10^{-9}	170	219	2.4	37	13	28
5	10	3.4×10^{-9}	202	437	2.3	41	13	34
	60	2.8×10^{-9}	184	398	2.5	42	13	33
	100	2.8×10^{-9}	184	398	2.5	42	13	33
10	10	4.1×10^{-9}	223	891	2.1	34	25	35
	60	3.2×10^{-9}	196	871	2.1	34	25	35
	100	3.2×10^{-9}	196	871	2.1	34	25	35

[a]The mean aperture and standard deviation are geometric mean and geometric standard deviation of local apertures, respectively.

displacements of 0 and 3 mm (Figure 8). In addition, the anisotropy of the spatial correlation lengths was observed for shear displacements greater than 1 mm. The spatial correlation lengths perpendicular to shear displacement were greater than those that were parallel to shear displacement. The anisotropy tended to increase with an increase in shear displacement.

[22] For higher confining pressures, the histograms moved to the left and mean apertures became smaller in the same trends of decreasing fracture permeability with increasing confining pressure. Correspondingly, the contact areas increased. On the other hand, the correlation lengths remained the same.

[23] Water flow in the aperture structures is depicted in Figure 4. The images show the distributions of local flow rates normalized with the maximum values for each aperture structure. To distinguish between local flow rates, which usually ranged from unity to values considerably less than unity, the relatively high local flow rates (1–0.001) observed for all aperture structures are indicated by gray scale, while the remaining smaller local flow rates (<0.001) are indicated in black.

[24] Comparing the images of aperture structures and water flow for a confining pressure of 10 MPa, the magnitudes of local apertures did not always correspond to those of local flow rates. The development of preferential flow paths, which was characterized as having a relatively high flow rate in limited regions, was observed. For different shear displacements, differences in the development of the preferential flow paths were observed depending on differences in the aperture structures. For example, the area of the preferential flow paths for a shear displacement of 1 mm was considerably larger than that observed for a shear displacement of 0 mm. These disparities were reflected by the differences in the relationship between hydraulic and mean apertures (Figure 9). Although the ratios of the hydraulic apertures to the mean apertures were always less than unity, the ratios increased for shear displacements of between 0 and 1 mm and subsequently decreased with an increase in shear displace

[25] The development of preferential flow paths, as well as changes within these paths, was also observed at higher confining pressures. However, despite the occurrence of the same changes in the aperture structures (i.e., uniform reduction of all local apertures), the changes differed in response to differences in shear displacement. For example, the area of preferential flow paths for a shear displacement of 0 mm increased between confining pressures of 10 and 60 MPa, whereas the area of preferential flow paths decreased when the shear displacement was 1 mm. Despite different changes in the area of preferential flow paths with increasing confining pressure, the ratio of hydraulic aperture to mean aperture at all shear displacements decreased.

5. Discussion and Conclusions

[26] The objectives of the present study were to propose a practical numerical technique for investigating aperture

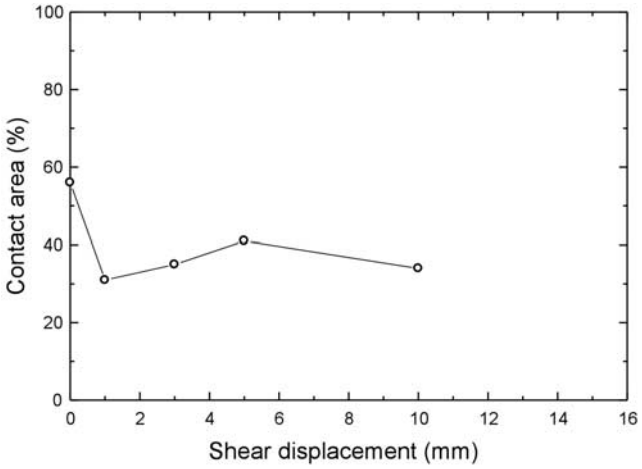

Figure 7. The nonmonotonic changes in the contact area with increasing shear displacement for numerically determined aperture structures at a confining pressure of 10 MPa for artificially created granite tensile fractures.

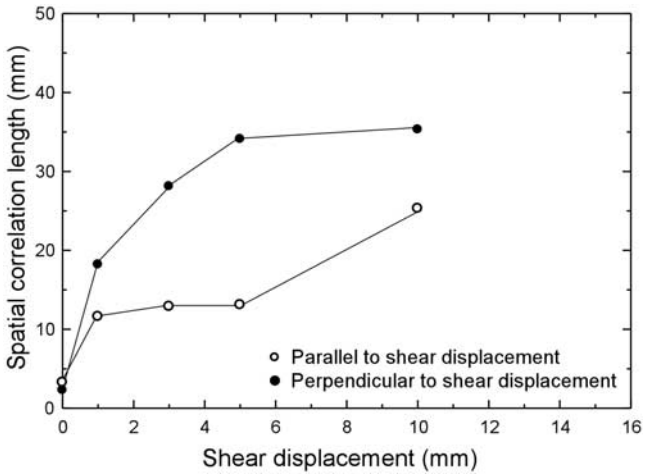

Figure 8. The nonmonotonic changes of the spatial correlation lengths in the directions parallel and perpendicular to shear displacement with increasing shear displacement for numerically determined aperture structures at a confining pressure of 10 MPa for artificially created granite tensile fractures.

structures and the resulting fluid flow through rock fractures under various confining pressures by incorporating the results of a flow-through experiment. In doing so, we sought to obtain fundamental insights into the heterogeneous nature of aperture and flow structures of rock fractures with respect to various geological conditions, including relatively high confining pressures of 10–100 MPa. The novelty of the proposed technique lies in the incorporation of experimental measurements of fracture permeability into a numerical model, which is itself based on the most practical numerical methods (individual measurement of fracture surfaces, a 2-D flow-through simulation based on the LCL, and a simulation of normal displacement ignoring deformation of fracture surfaces, except for contacting asperities). However, the numerical modeling methods employed in the present study were relatively rudimentary when compared with those reported in recently published studies, as described in section 3. Here, the relevance of the obtained results was evaluated using physical data from other rock fractures before fluid flow in the aperture structures of rock fractures under the confining pressures was discussed.

[27] Since the primary goal of the proposed technique was to model the permeability of an aperture structure with an experimentally determined fracture permeability under normal displacement and flow-through conditions, one method for evaluating the relevance of the obtained results could be to assess the relevance of contact areas in determined aperture structures. The aperture structures in the present study were represented using 2-D distributions of local apertures in 250 μm square grid systems, and the contact areas were percentages of minimum local apertures (1 μm-local apertures) for all local apertures in the aperture structures. The contact areas ranged between approximately 31% and 56% at a confining pressure of 10 MPa (Table 1). Conversely, *Montemagno and Pyrak-Nolte* [1999] determined the aperture structures in a 300 μm square grid system for fractures in coal using Wood's metal injection method combined with X-ray CT. They demonstrated that the contact areas (percentages of local apertures less than 2 μm for all local apertures) ranged between 42% and 55% at a confining pressure of 5 MPa. Given the similarities in spatial resolution between the definitions for the contact area and confining pressure in the present and previous studies, the contact areas in the present study appear reasonable when compared with those reported previously. In addition, the contact area in the present study did not change significantly with an increase in shear displacement (Figure 7), and the nonmonotonic changes of the contact area were consistent with changes in shear stress (existence of constant residual shear stress) observed in granite fractures during the shear process under similar normal stresses (confining pressures) [*Esaki et al.*, 1999]. Although further evaluations are required, no comparable physical data of aperture structures under conditions similar to those of the present study currently exists. At present, it appears that the results obtained using the proposed technique and numerical methods are reasonable.

[28] The results of the flow-through experiments for the fractures indicated that fracture permeability was usually considerably greater than matrix permeability, even at a confining pressure of 100 MPa (Figure 2). Consequently, it is expected that natural rock fractures may play dominant roles in subsurface flow, even under confining pressures exceeding 100 MPa. Although relatively high confining pressures have not been considered in previous studies associated with water resources issues, the experimental results illustrate the importance of understanding fluid flow in the aperture structures of rock fractures under high confining pressures in order to understand the regional groundwater flow system. The numerical results in the present study can provide fundamental insights into the heterogeneities associated with the aperture structures and the fluid flow within them under various geological conditions. The development of preferential flow paths was clearly observed in every aperture structure (Figure 4),

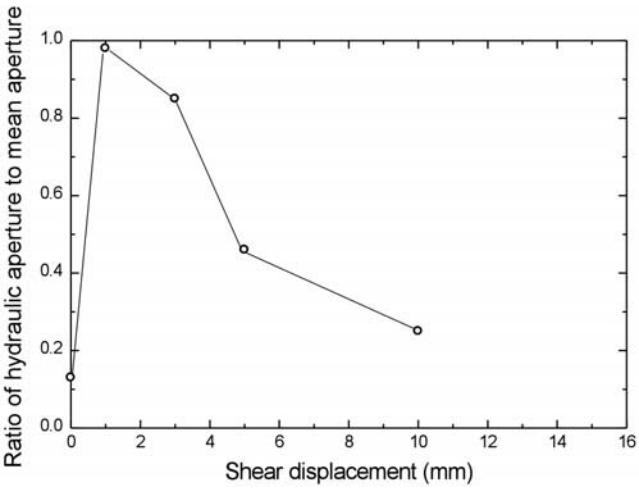

Figure 9. The nonmonotonic changes of the ratio of hydraulic aperture to the mean aperture with increasing shear displacement for numerically determined aperture structures at a confining pressure of 10 MPa for artificially created granite tensile fractures.

suggesting that the concept of channeling flow is applicable for rock fractures, even under a wide range of confining pressures, and that 3-D preferential flow paths can exist in a subsurface fracture network. In order to understand fluid flow structure and its significance, channeling flow should therefore be carefully investigated as a function of geological condition (shear displacement, confining pressure, etc.) because significant differences in preferential flow paths can arise due to heterogeneities that exist within the aperture structures. The proposed technique is expected to be suitable for lab-scale investigations of channeling flow. However, since lab-scale rock fractures as described in the present study were small, permanent deformation (crushing) of contacting asperities may be more likely to occur than in larger natural rock fractures in the field [*Raven and Gale*, 1985]. The magnitudes of permeability, aperture structures, and flow structures of the natural rock fractures can therefore be different from those of the rock fractures in the present study. Lab-scale rock fractures do not adequately represent all natural rock fractures, and size effects on fluid flow through rock fractures are still considered to be a fundamental problem [*Koyama et al.*, 2006; *Matsuki et al.*, 2006]. Nonetheless, the proposed technique for analyzing rock fractures of various sizes under various geological conditions can contribute to a better understanding of the heterogeneous nature of fluid flow in aperture structures of natural rock fractures and realistic regional groundwater system in the Earth's crust.

[29] **Acknowledgments.** The authors would like to thank Kazuhiko Tezuka, Tetsuya Tamagawa (Japan Petroleum Exploration Co., Ltd.), and Kimio Watanabe (Rich Stone Limited) for their assistance in the flow-through simulations using the D/SC.

References

Bertels, S. P., D. A. DiCarlo, and M. J. Blunt (2001), Measurement of aperture distribution, capillary pressure, relative permeability, and in situ saturation in a rock fracture using computed tomography scanning, *Water Resour. Res.*, *37*(3), 649–662.

Brown, S. R. (1987), Fluid flow through rock joints: The effect of surface roughness, *J. Geophys. Res.*, *92*(B2), 1337–1347.

Brown, S., A. Caprihan, and R. Hardly (1998), Experimental observation of fluid flow channels in a single fracture, *J. Geophys. Res.*, *103*(B3), 5125–5132.

Bruderer-Weng, C., P. Cowie, Y. Bernabé, and I. Main (2004), Relating flow channeling to tracer dispersion in heterogeneous network, *Adv. Water Resour.*, *27*(8), 843–855.

Brush, D. J., and N. R. Thomson (2003), Fluid flow in synthetic rough-walled fractures: Navier-Stokes, Stokes, and local cubic law assumptions, *Water Resour. Res.*, *39*(4), 1085, doi:10.1029/2002WR001346.

Chen, Z., S. P. Narayan, Z. Yang, and S. S. Rahman (2000), An experimental investigation of hydraulic behavior of fractures and joints in granitic rock, *Int. J. Rock Mech. Min. Sci.*, *37*(7), 1061–1071.

Durham, W. B. (1997), Laboratory observations of the hydraulic behavior of a permeable fracture from 3800 m depth in the KTB pilot hole, *J. Geophys. Res.*, *102*(B8), 18,405–18,416.

Esaki, T., S. Du, Y. Mitani, K. Ikusada, and L. Jing (1999), Development of a shear-flow test apparatus and determination of coupled properties for a single rock joint, *Int. J. Rock Mech. Min. Sci.*, *36*(5), 641–650.

Ge, S. (1997), A governing equation for fluid flow in rock fractures, *Water Resour. Res.*, *33*(1), 53–61.

Gutierrez, M., L. E. Øino, and R. Nygård (2000), Stress-dependent permeability of a de-mineralized fracture in shale, *Mar. Pet. Geol.*, *17*, 895–907.

Hakami, E., and E. Larsson (1996), Aperture measurements and flow experiments on a single natural fracture, *Int. J. Rock Mech. Min. Sci. Geochem. Abstr.*, *33*(4), 395–404.

Hirano, N., N. Watanabe, and N. Tsuchiya (2005), Development of rubber confining pressure vessel and flow test using this apparatus, *J. Min. Mater. Processes Inst. Jpn.*, *121*, 484–488 (in Japanese with English abstract).

Konzuk, J. S., and B. H. Kueper (2004), Evaluation of cubic law based models describing single-phase flow through a rough-walled fracture, *Water Resour. Res.*, *40*, W02402, doi:10.1029/2003WR002356.

Kostakis, K., J. P. Harrison, and S. M. Heath (2003), Silicone rubber casting for aperture measurement of rock fractures, *Int. J. Rock Mech. Min. Sci.*, *40*(6), 939–945.

Koyama, T., N. Fardin, L. Jing, and O. Stephanson (2006), Numerical simulation of shear-induced flow anisotropy and scale dependent aperture and transmissivity evolution of rock fracture replica, *Int. J. Rock Mech. Min. Sci.*, *43*(1), 89–106.

Lespinasse, M., and J. Sausse (2000), Quantification of fluid flow: Hydro-mechanical behavior of different natural rough fractures, *J. Geochem. Explor.*, *69–70*, 483–486.

Matsuki, K., Y. Chida, K. Sakaguchi, and P. W. J. Glover (2006), Size effect on aperture and permeability of a fracture as estimated in large synthetic fractures, *Int. J. Rock Mech. Min. Sci.*, *43*(5), 726–755.

Montemagno, C. D., and L. J. Pyrak-Nolte (1999), Fracture network versus single fractures: Measurement of fracture geometry with X-ray tomography, *Phys. Chem. Earth Part A*, *24*(7), 575–579.

Mourzenko, V. V., J.-F. Thovert, and P. M. Adler (1995), Permeability of a single fracture: Validity of the Reynolds equation, *J. Phys. II*, *5*(3), 465–482.

Olsson, R., and N. Barton (2001), An improved model for hydromechanical coupling during shearing of rock joints, *Int. J. Rock Mech. Min. Sci.*, *38*(3), 317–329.

Oron, A. P., and B. Berkowitz (1998), Flow in rock fractures: The local cubic law assumption reexamined, *Water Resour. Res.*, *34*(11), 2811–2825.

Plouraboué, F., P. Kurowski, J. M. Boffa, J. P. Hulin, and S. Roux (2000), Experimental study of the transport properties of rough self-affine fractures, *J. Contam. Hydrol.*, *46*(3), 295–318.

Polak, A., D. Elsworth, J. Liu, and A. S. Grader (2004), Spontaneous switching of permeability changes in limestone fracture with net dissolution, *Water Resour. Res.*, *40*, W03502, doi:10.1029/2003WR002717.

Power, W. L., and W. B. Durham (1997), Topography of natural and artificial fractures in granitic rocks: Implication for studies of rock friction and fluid migration, *Int. J. Rock Mech. Min. Sci.*, *34*(6), 979–989.

Pyrak-Nolte, L. J., and J. P. Morris (2000), Single fractures under normal stress: The relation between fracture specific stiffness and fluid flow, *Int. J. Rock Mech. Min. Sci.*, *37*(1–2), 245–262.

Raven, K. G., and J. E. Gale (1985), Water flow in a natural rock fracture as a function of stress and sample size, *Int. J. Rock Mech. Min. Sci.*, *22*(4), 251–261.

Sausse, J. (2002), Hydromechanical properties and alteration of natural fracture surfaces in the Soultz granite (Bas-Rhin, France), *Tectonophysics*, *348*(1), 169–185.

Takahashi, M., A. Hirata, and H. Koide (1990), Effect of confining pressure and pore pressure on permeability of Inada granite, *J. Jpn. Soc. Eng. Geol.*, *31*(3), 1–10 (in Japanese with English abstract).

Tezuka, K., and K. Watanabe (2000), Fracture network modeling of Hijiori hot dry rock reservoir by deterministic and stochastic crack network simulator (D/SC), in *Proc. World Geotherm. Cong. 2000*, pp. 3933–3938, International Geothermal Association.

Tsang, Y. W., and C. F. Tsang (1989), Flow channeling in a single fracture as a two-dimensional strongly heterogeneous permeable medium, *Water Resour. Res.*, *25*(9), 2076–2080.

Tsuchiya, N., and K. Nakatsuka (1995), Fractal analysis and modeling of a two-dimensional fracture network in a geothermal reservoir, *Geotherm. Resour. Counc.*, *19*, 547–552.

Tsuchiya, N., and K. Nakatsuka (1996), A two-dimensional mono-fractal approach to natural fracture networks in rocks, *Geotherm. Sci. Technol.*, *6*(1–4), 63–82.

Unger, A. J. A., and C. W. Mase (1993), Numerical study of the hydromechanical behavior of two rough fracture surfaces in contact, *Water Resour. Res.*, *29*(7), 2101–2114.

van Genabeek, O., and D. H. Rothman (1999), Critical behavior in flow through a rough-walled channel, *Phys. Lett. A and B*, *255*(1–2), 31–36.

Watanabe, N., N. Hirano, T. Tamagawa, K. Tezuka, and N. Tsuchiya (2005), Numerical estimation of aperture structure and flow wetted field in rock fracture, *Geotherm. Resour. Counc.*, *29*, 431–436.

Watanabe, N., N. Hirano, T. Tamagawa, K. Tezuka, and N. Tsuchiya (2006a), High resolution modeling of aperture structure and flow path in rock fracture, in *WATER DYNAMICS: 3rd International Workshop on Water Dynamics*, *AIP Conf. Proc.*, vol. 833, edited by K. Tohji et al., pp. 173–176, AIP, New York.

Watanabe, N., N. Hirano, T. Tamagawa, K. Tezuka, and N. Tsuchiya (2006b), Fundamental study for prediction of productivity in oil/gas fractured reservoir based on flow-through experiment under confining pressure, *J. Jpn. Assoc. Petrol. Technol.*, *71*(2), 217–226 (in Japanese with English abstract).

Watanabe, N., N. Hirano, and N. Tsuchiya (2006c), Experimental evaluation of fluid flow through artificial shear fracture in granite, *Geotherm. Resour. Counc.*, *30*, 361–366.

Yasuhara, H., A. Polak, Y. Mitani, A. S. Grader, P. M. Halleck, and D. Elsworth (2006), Evolution of fracture permeability through fluid-rock reaction under hydrothermal conditions, *Earth Planet. Sci. Lett.*, *244*, 186–200.

Yeo, I. W., M. H. deFreitas, and R. W. Zimmerman (1998), Effect of shear displacement on the aperture and permeability of a rock fracture, *Int. J. Rock Mech. Min. Sci.*, *35*(8), 1051–1070.

N. Hirano, N. Tsuchiya, and N. Watanabe, Graduate School of Environmental Studies, Tohoku University, 6-6-20 Aramaki-aza-Aoba, Aoba-ku, Sendai, Miyagi 980-8579, Japan. (watanabe@geo.kankyo.tohoku.ac.jp)